ELSEVIER

Catalysis Today 79–80 (2003) 195–202

CATALYSIS TODAY

www.elsevier.com/locate/cattod

Explaining mass transfer observations in multiphase stirred reactors: particle-liquid slip velocity measurements using PEPT

R.P. Fishwick [a], J.M. Winterbottom [a,*], E.H. Stitt [b]

[a] *Catalysis and Reaction Engineering Group, Department of Chemical Engineering, The University of Birmingham, Edgbaston, Birmingham B15 2TT, UK*

[b] *Synetix, P.O. Box 1, Belasis Avenue, Billingham, Cleveland TS23 1LB, UK*

Abstract

Solid–liquid mass transfer coefficients were determined using the technique of dissolving a sparingly soluble solid, salicylic acid loaded onto silica, in water. Mass transfer was found to be dependent on various particle characteristics. Of particular interest is the influence of the particle-liquid density difference. It is suggested that the change in mass transfer coefficient with these parameters is related, to some extent, with the particle-liquid slip velocity. The technique of positron emission particle tracking (PEPT) has been used in parallel with the mass transfer measurements in order to study the effect of different operating conditions on the liquid flow patterns and the particle-liquid slip velocities. Using PEPT, time-averaged slip velocities were determined by simple subtraction of the data from a neutrally buoyant particle. In this way, important information about solid–liquid behaviour and zones of poor mass transfer in stirred vessels is revealed.

Keywords: Multiphase reactors; Stirred vessels; Mass transfer; Hydrodynamics; Visualisation; Slip velocity

1. Introduction

Multiphase mechanically agitated reactors are of significance in a wide variety of processes such as the hydrogenation and oxidation of many fine and bulk chemicals, hardening of unsaturated oils as well as aerobic fermentations and waste treatment [1]. Catalytic reactions in stirred vessels involve processes such as gas–liquid mass transfer, solid–liquid mass transfer, intraparticle diffusion, adsorption, surface reaction and desorption of the products, making it a highly complicated system. Clearly, it is important to understand these processes and the effect of the system hydrodynamics when designing reactors. The objective of this study was to study the effect of the particle characteristics on solid–liquid mass transfer and mixing. This is of particular importance in mass transfer limited reactions such as frequently occurs with hydrogenation reactions where hydrogen is apt to be consumed faster than it can be supplied to the catalyst surface. Solid–liquid mass transfer in agitated vessels has been widely studied [2–5] and is not discussed here. The effect of the particle-fluid density difference, however, has been largely ignored. Indeed most empirical correlations completely omit particle density. It is also important to understand flow patterns and velocities in stirred vessels. In addition to good bulk fluid motion, adequate local velocities in parts of the vessel remote from the impeller are important in order to reduce resistance to mass transfer as well as to achieve good suspension and dispersion of the particles. Solid–liquid mass transfer has been suggested

* Corresponding author.
E-mail address: j.m.winterbottom@bham.ac.uk (J.M. Winterbottom).

0920-5861/03/$ – see front matter
doi:10.1016/S0920-5861(03)00005-1

Nomenclature

C	impeller clearance (m)
d_a	diameter of the agitator (m)
D_T	vessel diameter (m)
h	vertical position (m)
H	liquid height in vessel (m)
k_S	solid–liquid mass transfer coefficient ($m\,s^{-1}$)
N	agitator speed (s^{-1})
Q_G	gas flow rate ($m^3\,s^{-1}$)
r	radial position (m)
R	radius of vessel (m)
Re_I	impeller Reynolds number, dimensionless
St	Stokes number, dimensionless
v_{slip}	particle-liquid slip velocity ($m\,s^{-1}$)

Greek Letters

ρ_S	particle density ($kg\,m^{-3}$)
$\Delta\rho$	particle-liquid density difference ($kg\,m^{-3}$)
τ_f	fluid response time (s)
τ_p	particle response time (s)

to depend on the relative particle-liquid velocity. This slip velocity is, however, difficult to estimate. In the past, it has been suggested that at the point the particles are just suspended the slip velocity is of the order of the terminal velocity and that for higher agitation speeds a correction factor could be applied [6]. This approach has proved to be unsatisfactory, the possible reason being the wide variation in slip velocity that occurs in a vessel. Clearly, the variation in slip velocity can be problematic. Zones of relatively low slip velocity and hence mass transfer can arise, resulting in ineffective use of the vessel volume. This can clearly lead to problems when scaling-up vessels.

In order to study the liquid flow patterns and slip velocities the technique of positron emission particle tracking (PEPT) has been used to study the effects of the particle characteristics. PEPT is able to track a small radioactively labelled particle at speeds up to $10\,m\,s^{-1}$. The penetrative γ-rays employed in PEPT permit the accurate location of the tracer in opaque systems or even inside actual engineering equipment and has previously been used to study particle behaviour in systems such as mixers and fluidised beds [7] but only recently tested in stirred vessels [8]. A consequence of this is that gassed systems can be studied without the difficulties sometimes experienced with optical techniques such as particle imaging velocimetry (PIV) and laser doppler anemometry (LDA) where diffraction can be problematic. The use of neutrally buoyant γ-ray emitting particle tracking for studying mixing patterns in single-phase vessels has recently been reported and validated [8,9]. Using PEPT with tracers of selected characteristics therefore reveals the effect of the system on the liquid flow patterns and the solid–liquid slip velocities.

2. Experimental

2.1. The stirred vessel

The reactions were conducted in a glass, cylindrical, flat-bottomed vessel fitted with four 10% baffles as described in Fig. 1. The diameter of the vessel is 0.1 m giving a vessel volume of approximately 0.67 dm^3 when filled to a height equal to the vessel diameter.

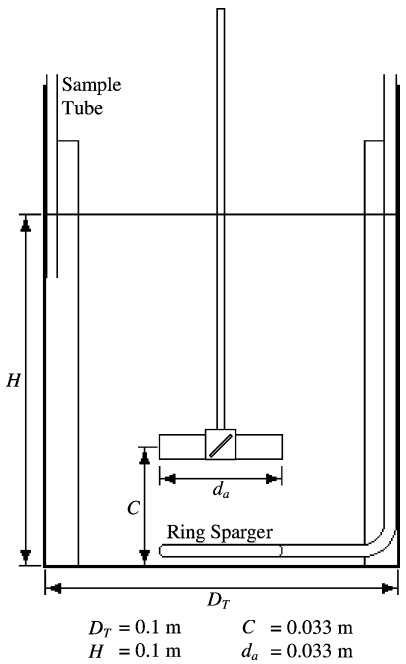

Fig. 1. The stirred vessel.

A pitched blade turbine was located one-third of the vessel diameter from the bottom of the tank. For these studies, a relatively dilute particle concentration of 1% (v/v) was utilised and the system was maintained at atmospheric pressure and a temperature of 25 °C by immersion of the vessel in a water bath.

2.2. Solid–liquid mass transfer measurements

The solid–liquid mass transfer coefficient, k_S, was determined by the widely used method of dissolution of a sparingly soluble solid [3,10]. For this study salicylic acid, loaded onto silica gel granules, was dissolved in water. These particles were prepared by first dissolving the salicylic acid in ether followed by incipient wetness impregnation of the silica. Recrystalization of the acid onto silica gel produced particles ranging from 180 to 250 μm in diameter. The particle density was altered by the modification of some particles by the addition of lead sulfate or lead oxide into the porous silica. Salicylic acid was then recrystalized around this central core.

The rate of reaction was determined by titrating samples taken at regular intervals against 0.01N sodium hydroxide solution using a phenolphthalein indicator. A vacuum sampling system allowed small quantities of the solution to be withdrawn at relatively short time intervals. By passing the sample through a filter to remove any silica gel/salicylic acid particles further reaction was prevented so that the samples could be tested after the completion of the experiment.

2.3. Positron emission particle tracking

The technique of positron emission particle tracking (PEPT) enables a single radioactive tracer particle to be accurately tracked inside equipment. The weakly radioactive source decays with the emission of a positron, which are readily annihilated by electrons. Energy is released in the form of two back-to-back γ-rays, 180° apart to within about 0.5. The detectors are then able to detect the incident γ-rays and determine their interaction co-ordinates to within a few millimetres (Fig. 2). The system only records coincidence events in which gamma rays are detected at both detectors within a resolving time of 7.5 ns. From a small number of such events the tracer position can be determined by triangulation, resulting in the location of the particle. Sufficient events are used in order to determine erroneous results that occur, for example, when the γ-rays are scattered. The spatial resolution depends on various factors, predominantly the tracer speed. At a speed of $1\,m\,s^{-1}$ the tracer will be typically recorded 250 times per second and located to within 0.5 mm. A slower moving tracer can be located at a higher resolution by recording its position at a lower frequency. The present camera can track over a volume of $0.8\,m \times 0.5\,m \times 0.4\,m$ although accurate tracking is difficult near the extremes of this field of view. The PEPT technique is discussed in more detail by Parker et al. [11] and Parker and McNeil [12].

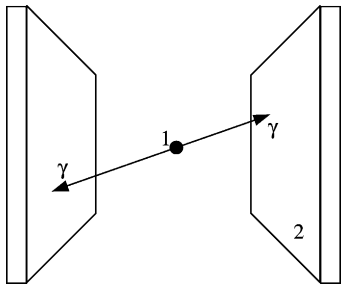

Fig. 2. Detection of gamma rays with positron emission particle tracking: 1, tracer particle; 2, dual headed gamma camera.

The neutrally buoyant and low-density tracers (approximately $1500\,kg\,m^{-3}$) were prepared from porous resin beads 200 μm in diameter, with water frozen inside the pores. The particles are then coated with a thin layer of paint to seal in the water. The higher density tracers (approximately $3000\,kg\,m^{-3}$) were prepared from haptite also coated in paint. The particles are then irradiated in a cyclotron with a ^3He beam to produce the positron-emitting radionuclide ^{18}F (half-life 110 min).

The question arises as to whether the particle can faithfully trace the fluid motion. Particle motion within a fluid of rapidly changing velocity is often characterised by the use of the Stokes number. The Stokes number is the ratio of the particle response time, τ_p and the fluid response time, τ_f (to an external disturbance, in this case the impeller) based on impeller diameter and impeller tip velocity. Equilibrium flow conditions can be assumed for $St < 0.1$ [13]. For these experiments, taking the worst case of $N = 800\,min^{-1}$, and assuming that the flow is Stokesian a Stokes number of the order of 0.092 is obtained in the vicinity of the

impeller where velocities are highest and τ_f is at its lowest. For the majority of the vessel lower values of *St* are expected. The neutrally buoyant tracer particle therefore should faithfully follow the fluid motion.

3. Results and discussion

3.1. Effect of the particle-liquid density difference on the solid–liquid mass transfer coefficient

Although a Reynolds number based either on the minimum particle suspension speed [14] or particle terminal velocity [6] may take the particle-fluid density difference into account to some extent, density appears not to have been widely investigated in the literature. The results obtained in this investigation using an upward pumping, pitched blade turbine are reported in Fig. 3 as mass transfer coefficient versus the particle density, ρ_S. Blasinski and Pyc [15] proposed the correlation $k_S \propto \rho_S^{0.25}$ for a two-phase system. Fig. 3 suggests the correlation $k_S \propto \rho_S^{0.252}$ for the two-phase system and $k_S \propto \rho_S^{0.255}$ for the gassed system. This is in good agreement and indicates that the influence of particle density is largely independent of gassing. Evidently, denser particles can achieve higher mass transfer rates and considering the range of solid catalysts in industrial use and their varying densities, the density difference would appear to be an important factor. It may be possible, therefore, to improve mass transfer simply by using heavier, denser catalysts.

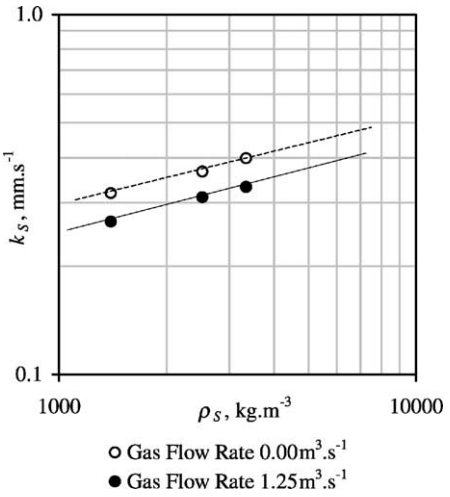

Fig. 3. Effect of particle density on solid–liquid mass transfer at 1% (v/v) solid concentration.

3.2. Particle-liquid hydrodynamics

Inertia effects in dense particles would be expected to be more prominent with the particles slow to respond to rapid changes in the fluid velocities. Fig. 4 shows the azimuthally averaged velocity of a neutrally buoyant particle measured for the pitched blade turbine. The flow into the impeller is clearly axial, with the discharge at approximately 45° forming a highly agitated circulation loop in the lower half of the vessel. The upper limit of this loop is located at height of 0.5*D*. The eye of the loop is located at a height of 0.25*D* and radially at 0.25*D*. The upper region experiences relatively lower velocities with a recirculation loop centred at a height of 0.6*D* and again radially at 0.25*D*. The particle velocities are reported in Figs. 5 and 6 for the 1485 and 3009 kg m^{-3} tracer, respectively.

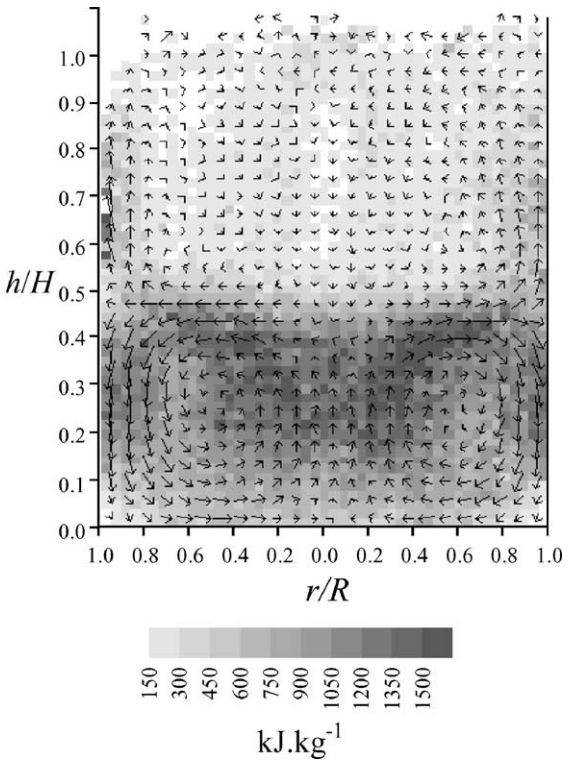

Fig. 4. Azimuthally averaged velocity vector and kinetic energy plot: pitched blade turbine stirred at 800 min^{-1}, neutrally buoyant, 250 μm tracer.

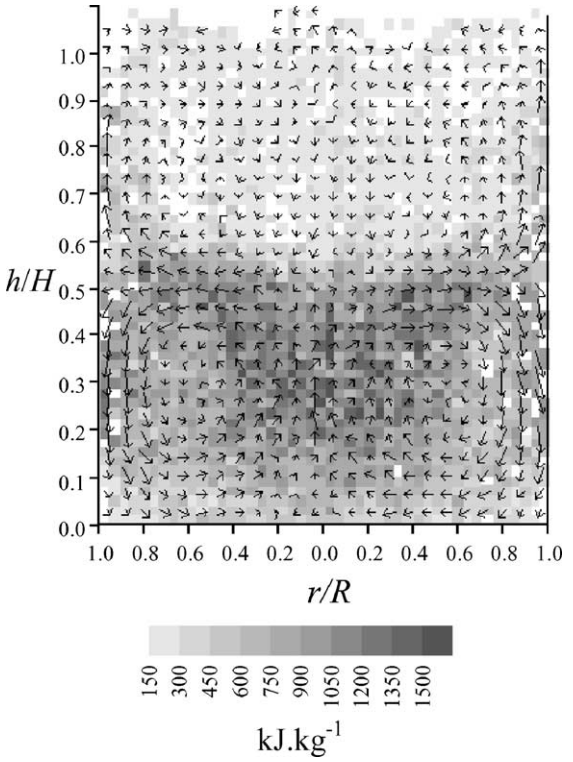

Fig. 5. Azimuthally averaged velocity vector and kinetic energy plot: pitched blade turbine stirred at 800 min^{-1}, 1485 $kg\,m^{-3}$, 250 μm tracer.

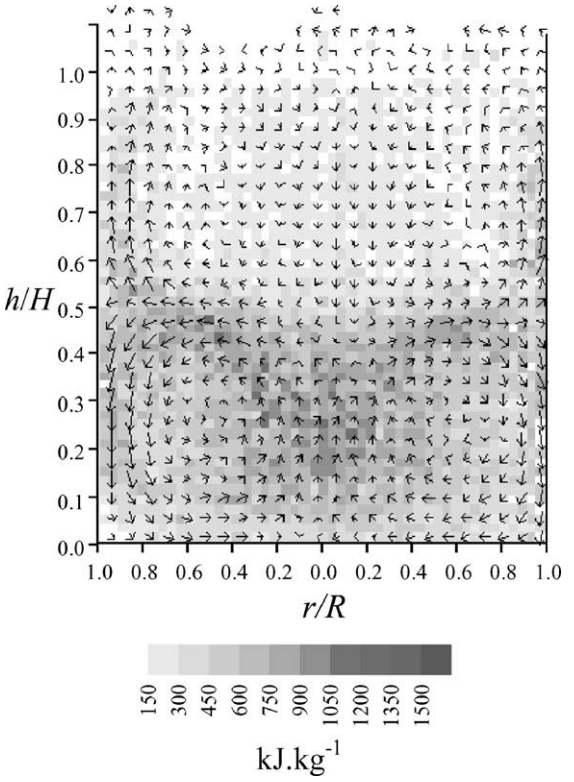

Fig. 6. Azimuthally averaged velocity vector and kinetic energy plot: pitched blade turbine stirred at 800 min^{-1}, 3009 $kg\,m^{-3}$, 250 μm tracer.

Comparing the three densities, the decrease in velocity of the tracer is particularly evident in the lower half of the vessel. However, the effect is less apparent in the upper half. This general decrease in velocity is further exemplified in Fig. 7, which shows the probability density function of tracer speed for the three densities. As the tracer density is increased there is a clear decrease in the velocity shown by the shift to the left. However, the curves display a clear shoulder, particularly with the lower densities, indicating a bi-modal distribution. The left-hand, lower velocity peak shows little change. By comparison, the greatest velocity change occurs in the right-hand, high velocity peak. Comparing with the velocities illustrated in Figs. 4–6 this suggests that the bi-modal distribution can be attributed to the upper and lower mixing loops. This can be demonstrated by analysing the two zones separately. Fig. 8, for the neutrally buoyant tracer, shows that the mean velocity of the liquid elements is found to be over twice as high in the lower mixing zone than the upper. This difference is reduced as the tracer density is increased, as it is mainly the lower region that is affected. The peak corresponding to the lower section shifts to lower velocities until, in the case of the highest density tracer, the shoulder disappears. In practical terms, this means considerably higher slip velocities occur in the lower region where the velocity gradients are highest. For a pitched blade turbine agitated at 800 min^{-1} an average relative slip velocity of 0.065 $m\,s^{-1}$ is observed with particles of 3009 $kg\,m^{-3}$ based on the mean tracer velocity. In the lower region, however, a slip velocity of 0.101 $m\,s^{-1}$ is found dropping to just 0.015 $m\,s^{-1}$ in the upper mixing zone.

3.3. The particle-liquid slip velocity

It is apparent that the particle-liquid slip velocity is influenced by the density difference and clearly considerable variation in the slip velocity occurs but is

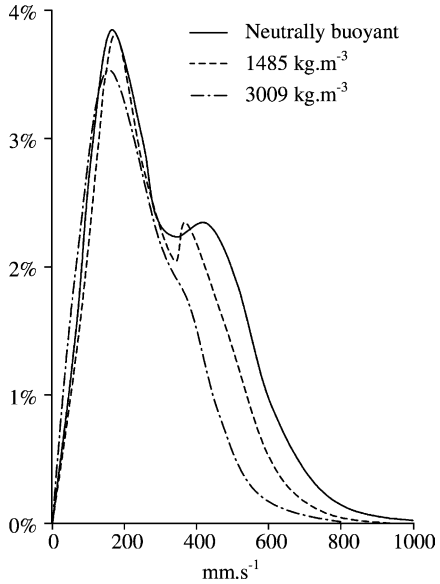

Fig. 7. Tracer velocity distribution: pitched blade turbine stirred at 800 min^{-1}, 250 μm tracer.

it in fact linked to the mass transfer coefficient? To some extent mass transfer at different slip velocities can be compared to mass transfer to free falling particles. The solid–liquid mass transfer coefficient is found to increase for particles with higher densities and hence higher terminal velocities [16,17]. However, in a chaotic system, such as a stirred vessel, inertia and momentum effects significantly accelerate the particle. Therefore, a direct comparison is difficult. Nevertheless, free falling particle mass transfer is at least suggestive of the effect of the relative particle-liquid velocity. As discussed previously, considerable variation in the slip velocity occurs in stirred vessels, being particularly high in the vicinity of the impeller (Figs. 4–6). This is confirmed in Fig. 9, which shows the variation in slip velocity throughout the vessel. The highest slip velocities are observed in the impeller discharge where the lowest resistance to mass transfer will occur. By comparison, the slip velocities are relatively small in the upper half of the vessel, although slightly higher around the baffles where the fluid velocity changes rapidly. Similar observations are also found along the bottom of the vessel and therefore mass transfer coefficients will be relatively low in these regions. The maldistribution of slip velocities is further illustrated in Fig. 10, which shows the probability density function

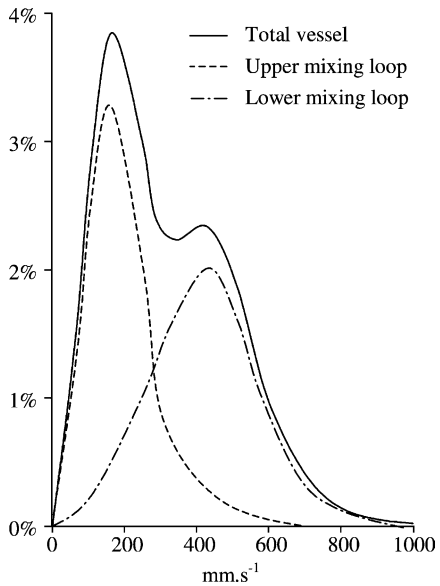

Fig. 8. Tracer velocity distribution: pitched blade turbine stirred at 800 min^{-1}, neutrally buoyant, 250 μm tracer.

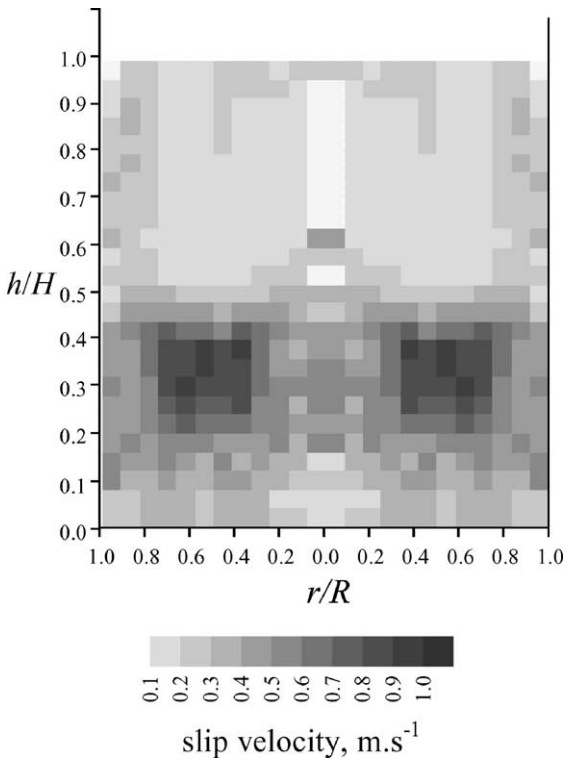

Fig. 9. Azimuthally averaged slip velocity plot: pitched blade turbine stirred at 800 min^{-1}, 3009 kg m^{-3}, 250 μm tracer.

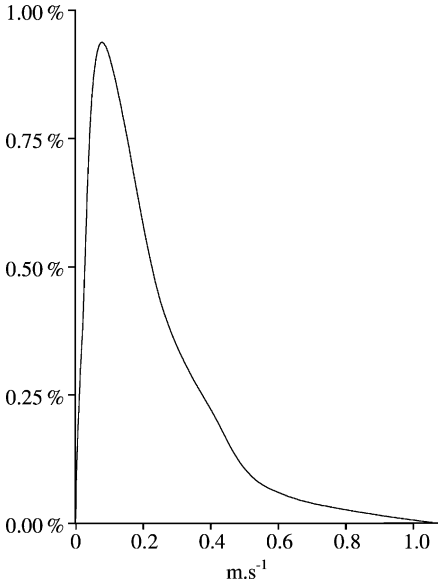

Fig. 10. Slip velocity distribution: pitched blade turbine stirred at 800 min^{-1}, 3009 $kg\,m^{-3}$, 250 μm tracer.

of v_{slip}. Clearly, the large majority of the vessel experiences significantly lower slip velocities than at the maximum of around 1 $m\,s^{-1}$. The slip velocity is below 0.2 $m\,s^{-1}$ in 50% of the vessel and below 0.5 $m\,s^{-1}$ in 90%. The non-uniformity in slip velocity will be even more problematic in large-scale reactors where the region of high shear will occupy a smaller proportion of the vessel. This will result in high mass transfer coefficients being confined to an even smaller portion of the vessel. This inadequate use of the vessel may explain to some extent some of the problems that can occur when scaling-up stirred tank reactors. Clearly, it is necessary to increase the velocity gradients in the stirred vessel, particularly for mass transfer limited reactions. Mass transfer may be improved, for example, by the use of draft tubes or multiple impellers to increase flow in the upper regions of the tank [18], although the latter will accompanied by larger power requirements.

4. Conclusions

Solid–liquid mass transfer is found to increase with increasing particle-liquid density difference and this is supported by studies of the hydrodynamics using PEPT. Considering the range of solid catalysts in industrial use it is clear that the significance of particle density cannot be overlooked when designing two and three-phase reactors. Ignoring the density effects on mass transfer and particle suspension could lead to an inadequately designed agitation system and hence, inefficient reactor, since it must be noted that large-scale vessels typically operate with much lower stirring speeds. Stirrer design in particular should be optimised. Further more, the slip velocity is found to be highest where the shear field gradients are at their greatest. Indeed, in half of the vessel slip velocities are below 20% of the maximum slip velocity. This high shear region will occupy a smaller proportion in large-scale reactors, therefore relatively high mass transfer coefficients may be expected to only occur in a small portion of the reactor. This highlights the problems that can occur when scaling-up an operation. While only a small diameter vessel has been used, and the observed effects occur primarily at low agitation rates, considerable non-uniformity of mass transfer in larger vessels is evident.

References

[1] R.V. Chaudhari, P.A. Ramachandran, AIChE J. 26 (1980) 177.
[2] F. Grisafi, A. Brucato, L. Rizzuti, Can. J. Chem. Eng. 76 (1998) 446.
[3] S. Boon-Long, C. Laguerie, J.P. Couderc, Chem. Eng. Sci. 33 (1978) 813.
[4] Y. Sano, N. Yamaguchi, T. Adachi, J. Chem. Eng. Jpn. 7 (1974) 255.
[5] D.M. Levins, J.R. Glastonbury, Trans. Inst. Chem. Eng. 50 (1972) 132.
[6] P. Harriott, AIChE J. 8 (1962) 93.
[7] M. Stein, T.W. Martin, J.P.K. Seville, P.A. McNeil, D.J. Parker, in: J. Chaouki (Ed.), Non-Invasive Monitoring of Multiphase Flows, Elsevier, Amsterdam, 1997, p. 161.
[8] Y.S. Fangary, M. Barigou, J.P.K. Seville, D.J. Parker, Chem. Eng. Sci. 55 (2000) 5969.
[9] A.R. Rammohan, A. Kemoun, M.H. Al-Dahhan, M.P. Dudukovic, Chem. Eng. Sci. 56 (2001) 2629.
[10] J.J. Barker, R.E. Treybal, AIChE J. 6 (1960) 289.
[11] D.J. Parker, C.J. Broadbent, P. Fowles, M.R. Hawkesworth, P. McNeil, Nucl. Instrum. Methods Phys. Res., A 326 (1993) 592.
[12] D.J. Parker, P. McNeil, Meas. Sci. Technol. 7 (1996) 287.
[13] J.A. Schetz, A.E. Fuhs, Handbook of Fluid Dynamics and Fluid Machinery, Wiley, New York, 1996, p. 906.

[14] K.B. Kushalkar, V.G. Pangarkar, Ind. Eng. Chem. Res. 33 (1994) 1817.
[15] H. Blasinski, K.W. Pyc, Int. Chem. Eng. 15 (1975) 73.
[16] K. Rahmant, M. Streat, Chem. Eng. Sci. 36 (1981) 301.
[17] R. Clift, J.R. Grace, M.E. Weber, Bubbles, Drops and Particles, Academic Press, New York, 1978, p. 97.
[18] A.W. Nienow, in: N. Harnby, M.F. Edwards, A.W. Nienow (Eds.), Mixing in the Process Industries, second ed., Butterworth-Heinemann, Oxford, 1992 (Chapter 16).